



Synthesis and Properties of Isoindigo and Benzo[1,2-b:4,5-b']bis[b]benzothiophene oligomers

Journal:	<i>ChemComm</i>
Manuscript ID	CC-COM-07-2018-005608.R2
Article Type:	Communication

SCHOLARONE™
Manuscripts

Synthesis and Properties of Isoindigo and Benzo[1,2-*b*:4,5-*b'*]bis[*b*]benzothiophene oligomers

Received 00th January 20xx,
Accepted 00th January 20xx

DOI: 10.1039/x0xx00000x

www.rsc.org/

Hailiang Liao,^a Chengyi Xiao,^b Mahesh Kumar Ravva,^{c,d} Yazhou Wang,^a Mark Little,^e Maud V C Jenart,^e Ada Onwubiko,^e Zhengke Li,^a Zhaohui Wang,^b Jean-Luc Brédas,^{c,f} Iain McCulloch,^{c,e} and Wan Yue^{*a,e}

A well-defined series of long and soluble isoindigo thienoacene oligomers have been synthesized from a novel electron deficient building block: benzo[1,2-*b*:4,5-*b'*]bis[*b*]benzothiophene bislactams. Extension of the π -conjugated systems facilitate control of optical, electronic and devices characteristics.

Aromatic units that possess electron deficient lactams are of significant interest as they could be incorporated into small molecules, oligomers and conjugated polymers, which have application in optical and electronic devices such as organic field-effect transistors, and photovoltaics.^{1,2,3} Of these lactams, isoindigo (IID) is one of the most versatile and extend used dye motif. IID comprises an electron deficient symmetrical bislactam, connected by a double bond, which could result in off-axis dipoles along the molecular backbone to promote intermolecular interactions. The lactam nitrogen of the IID provides a straightforward strategy toward alkylation to tune the solubility of the resulting materials. After it was recognized as a useful building block for making conjugated p-type oligomers for solar cells by Reynolds et al in 2010,⁴ IID and its core modified analogues, such as, TIID,⁵ TTIID,⁶ AIID,^{7,8} TBTI,⁹ DIID,^{10,11,12} BDOPV,¹³ have been reported and proven to be versatile building blocks for high performance polymer

semiconductors due to their fused aromatic rings and electron deficient lactams. Particularly, very recently McCulloch et al. reported fused electron deficient semiconducting polymers for air stable electron transport, the lactams incorporated into the polymer skeleton lead to high electron affinity to facilitate electron injection and transport.¹⁴

Additionally, thienoacenes are also versatile building blocks for the design of functional materials.^{15,16,17,18} The incorporation of thienoacene in functional materials can suppresses conformational disorder and lowers the charge-transfer reorganization energy. This low energetic disorder approach is expected to enhance charge carrier mobility.¹⁹ In addition, the planar π orbital skeleton minimizes the electronic band gap by extending the effective conjugation length.²⁰ For example, [1]Benzothieno[3,2-*b*]benzothiophene (BTBT) and its derivatives show very high charge carrier mobilities.²¹ Benzo[1,2-*b*:4,5-*b'*]bis[*b*]benzothiophene (BBBT, Figure 1a), has been employed as a p-channel semiconductor with thin-films fabricated from both vacuum deposition and drop casting.^{22,23}

Thus, thienoacene and isoindigo building blocks have inspired us to design and develop new zigzag multi lactams contained oligomers with good processability. These large π systems are locked into a rigid conformation by the exclusion of single linking bonds, thus unique optical and electronic properties and application as electronic functional materials are expected.

^a H. Liao, Y. Wang, Prof. Z. Li, Prof. W. Yue, Key Laboratory for Polymeric Composite and Functional Materials of Ministry of Education, School of Materials and Engineering, Sun Yat-Sen University, Guangzhou 510275, China. E-mail: yuew5@mail.sysu.edu.cn

^b Dr. C. Xiao, Prof. Z. Wang, CAS Research/Education Center for Excellence in Molecular Sciences Institute of Chemistry, Chinese Academy of Sciences, Beijing 100190, P. R. China

^c Dr. M. K. Ravva, Prof. J. L. Brédas, Prof. I. McCulloch, King Abdullah University of Science and Technology (KAUST), SPERC, Thuwal, 23955-6900, Saudi Arabia

^d Dr. M. K. Ravva, Department of Chemistry, SRM University – AP, Amaravati 522502, India

^e Dr. M. Little, Dr. J. Maud V C, A. Onwubiko, Prof. I. McCulloch, Prof. W. Yue, Department of Chemistry and Centre for Plastic Electronics, Imperial College London, South Kensington, London, SW7 2AZ, United Kingdom

^f Prof. J.L. Brédas, Center for Organic Photonics and Electronics, Georgia Institute of Technologies, Atlanta, Georgia 30332-0400, USA

† Footnotes relating to the title and/or authors should appear here.

Electronic Supplementary Information (ESI) available: [details of any supplementary information available should be included here]. See DOI: 10.1039/x0xx00000x

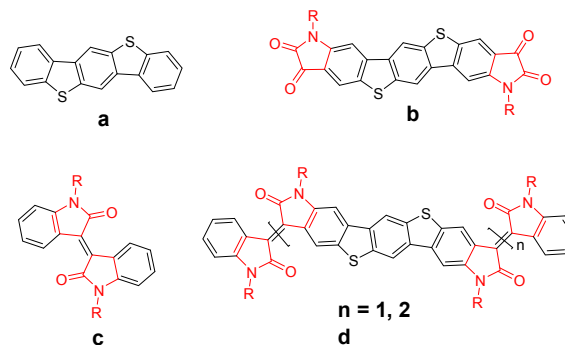


Figure 1. Chemical structures of benzo[1,2-*b*:4,5-*b'*]bis[*b*]benzothiophene (BBBT) (a), benzo[1,2-*b*:4,5-*b'*]bis[*b*]benzothiophene bislactams (b), isoindigo (c), and isoindigo-BBBT oligomers (d), R is 2-decyltetradecyl.

With these concepts in mind, we combined fused thienoacene BBT units (Figure 1a) with an electron withdrawing isoindigo unit (Figure 1b). Addition of an isoindigo unit not only increases the electron affinity (EA) due to the electron deficient lactams but also provides an opportunity to incorporate additional alkyl functionality. Therefore, this design strategy can simultaneously stabilize and solubilize the larger multi lactams. The larger π -conjugation length provides an increased area for intermolecular charge transfer, reduces the reorganization energy, and tunes the highest occupied molecular orbital (HOMO) and lowest unoccupied molecular orbital (LUMO) energy levels.²⁴

Herein, we report the systematic extension of the BBT-isoindigo multi lactams series comprising up to 18 rings. The strategy used for the synthesis begins with a novel electron deficient BBT bislactam **6**. Single or two-fold Knoevenagel condensation of BBT bislactam **6** with oxindole **7** affords the asymmetric 9-ring system **8** and the symmetric 11-ring **9**. Subsequent deoxygenated coupling of two 9-ring units results in formation of a soluble 18-ring system **10**.

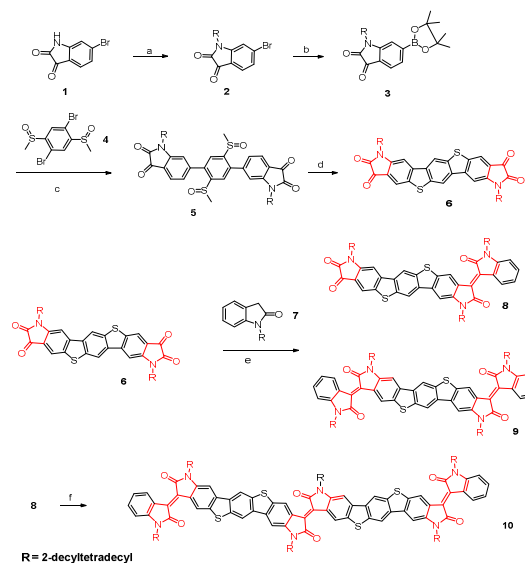
The synthetic pathway to the central BBT-bislactam unit **6** is portrayed in Scheme 1. First, the branched 2-decyltetradecyl chain was attached on the amide position from 6-bromoisatin **1** to ensure sufficient solubility. Pd-catalyzed Miyaura borylation between **2** and bis(pinacolato)diboron furnished **3** in a good yield, which then reacted with 1,4-dibromo-2,5-bis(methylsulfinyl)benzene **4**²⁵ under typical Suzuki reaction conditions, providing the intermediate 1,4-di((6-N-2-decyltetradecyl) isatin)-2, 5-bis(methylsulfinyl) benzene **5**. The final annulation step was performed by treatment of sulfoxide **5** with Eaton's reagent (phosphorus pentoxide/ methanesulfonic acid), followed by demethylation of the sulfonium salt, affording BBT-bislactam **6** in a moderate yield.^{26,27}

P-toluene sulfonic acid monohydrate (PTSA) catalyzed aldol condensation between **6** and N-decyltetradecyloxindole **7** (see SI for the synthesis route of **7**) affords compound **8** and compound **9** by controlling the stoichiometry of reactant **7**.²⁸ The longest 18-ring BBT-isoindigo **10** has been synthesized by deoxygenated coupling of **8** with hexaethyltriaminophosphine in dichloromethane (DCM) with an excellent yield without column chromatography purification. Note that all these fused zigzag multi lactams are prepared in a very atom economical way without the use of metal catalyst.

Compound **6** is moderately soluble in chloroform. Compounds **8**, **9**, and **10** have good solubility in common organic solvents, such as chloroform (CHCl₃) and toluene. The molecular structures have been confirmed by proton nuclear magnetic resonance (¹H NMR), carbon nuclear magnetic resonance (¹³C NMR) spectroscopy, and matrix-assisted laser desorption/ionization time-of-flight (MALDI-TOF) mass spectrometry. Figure S1 shows the partial aromatic region proton NMR of **8**, **9**, and **10**. Due to the asymmetrical structure of compound **8**, the six singlets of **8** were assigned to the protons of middle hetero rings BBT unit, the additional two doublets and two triplets were assigned to the flanking outward phenyl rings. In comparison, only three singlet peaks of **9** can be observed for the aromatic BBT unit due to its centrosymmetric structure. The proton and carbon NMR of **10** were obtained at a high temperature (403 K) in 1,1,2,2-tetrachloroethane-d₂. No peaks at room temperature could be observed in CDCl₃, despite good solubility, due to the very strong aggregation for this large aromatic system. Similarly, for compounds **8** and **9**, the six singlets in the aromatic region can also be assigned to the fused BBT rings, and the doublets and triplets can be assigned to the flanking phenyl rings. Note that the proton signal in compound **8** (8.01 ppm)

strongly shifted to 9.90 ppm for compound **10**, which could be ascribed to the deshielding effect of the carbonyl group.

Scheme 1. Synthesis of BBT bislactams and BBT-isoindigo multi-lactams.



Scheme 1. (a) 1-Bromo-2-decyltetradecane, K₂CO₃, dry DMF, 70 °C, 65%; (b) Bis(pinacolato)diboron, Pd(PPh₃)₂Cl₂, CH₃COOK, toluene, 90 °C, 85%; (c) 1,4-Dibromo-2,5-bis(methylsulfinyl)benzene **4**, Pd(PPh₃)₄, 2M K₂CO₃, 90 °C, 48%; (d) Eaton's reagent, room temperature, then pyridine, reflux, 35%; (e) **6** (1.2 equiv **6** for **8**), **7** (2.67 equiv **7** for **9**), PTSA, toluene, reflux, **8** (56%), **9** (62%); (f) hexaethyltriaminophosphine, DCM, -78 °C to rt, 92%.

The optical properties of these extended rings multi lactams were studied by UV-Vis absorption spectroscopy (Figure 2). These oligomers exhibit broad and intense absorption bands with corresponding broad tails with relatively low intensity in the low energy bands. In contrast with BBT, which only shows absorption in the UV region,^{22,23} compound **6** shows a significant bathochromic shift into the visible region with the peak of the first low energy absorption at 522 nm; the absorption tail extends to 650 nm due to interaction with the outward two electron deficient lactam rings. The absorption spectra of **8**, **9**, and **10** shift bathochromically with the increasing conjugated length of the aromatic units. Compound **8** exhibits a molar extinction coefficient (ϵ) of 36400 M⁻¹cm⁻¹ at 462 nm. In contrast, compound **9** exhibits a red shift absorption with ϵ of 61000 M⁻¹cm⁻¹ at 492 nm for compound **10**, a higher ϵ of 87300 M⁻¹cm⁻¹ at 514 nm is observed, which could be attributed to the extended conjugated length of aromatic units. Density functional theory calculations were carried out to understand the nature of these optical transitions. Geometry optimization of molecules **6**, **8**, **9** and **10** were performed at the ω B97XD/6-31G(d,p) level of theory. Optimized geometry of molecule **6** exhibits a completely co-planar conformation whereas molecules **8**, **9** and **10** show a small twist with a dihedral angle of 10^o~11^o between the two lactam units (Figure S2). This is due to the steric interactions between the oxygen atom of the carbonyl group and the neighboring hydrogen from the alpha C-H bond of the BBT fused rings, at a distance of 1.9 Å, and is observed in most isoindigo molecules.¹⁴ The vertical excited-state energies were calculated at the time dependent (TD)- omega tuned ω B97XD/6-31g(d,p) level of

theory. The calculated absorption spectra for these molecules are presented in Figure S3. The calculated excited-state energies of these molecules show similar trend with the experimental values. An analysis of the natural transition orbitals (NTO) for the lowest optical transitions for molecules **6**, **8**, **9**, and **10**, which are illustrated in Figure S4, reveals that the hole NTO mostly localizes on the central BBT region, while the electron NTO has most of its density on the lactam groups. Therefore, the low energy transition in molecules **8**, **9**, and **10** displays a partial intramolecular charge transfer (ICT) character and the relative lower intensity of the absorption could be attributed to this ICT character. The bands with high intensity of **8**, **9** and **10** are dominated by a $\pi-\pi^*$ electronic excitation (Figure S5). Therefore, the energy of this transition decreases gradually with the extension of the aromatic core by fusion of BBT and isoindigo units. The long absorption tails may be caused by intramolecular donor-acceptor charge transfer interaction from the electron rich BBT units to the electron deficient lactams. The onset optical gaps shift from 1.94 eV to 1.88 eV, 1.82 eV and 1.68 eV for compounds **6**, **8**, **9** and **10**, respectively (Table 1). In comparison to the solution spectra, the thin film absorption peak of the first low energy band is red shifted by 20 nm for **6** ($\lambda_{\text{max}} = 547$ nm); the lowest energy absorption bands of thin films of compounds **8**, **9** and **10** are also slightly red shifted (Figure S7, S8, S9, S10 and S11), suggesting J-aggregation in the solid state.²⁹

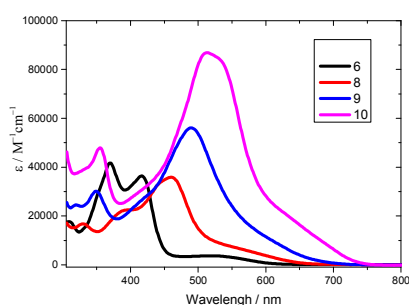


Figure 2. Absorption spectra of fused BBT bislactams and BBT-isoindigo oligomers **6**, **8**, **9** and **10** in CHCl_3 solution at room temperature.

The frontier molecular orbital energy levels and wavefunction distributions for **6**, **8**, **9** and **10** were calculated at OT(chloroform)- ω B97XD/6-31G(d,p) level of theory (Figure S6). Both HOMO and LUMO wavefunctions of **6** are delocalized over the whole molecule. In **8**, **9**, and **10**, the HOMO wavefunction mainly localizes on the central BBT region, while the LUMO wavefunction localizes on the indigo units.

Table 1: Optical and electrochemical properties of fused BBT-isoindigo oligomers **6, **8**, **9** and **10**.**

Comp.	ϵ^a [$\text{M}^{-1}\text{cm}^{-1}$]	λ_{onset}^b [nm]	E_{onset}^c [V]	E_{A}^d [eV]	E_{g}^e [eV]	IP^f [eV]	E_{g}^g [eV]	IP^h [eV]	E_{A}^i [eV]
6	36800	642	–	3.55	1.94	5.49	3.16	5.85	2.69
8	36400	663	1.25	3.58	1.88	5.46	2.91	5.59	2.68
9	56100	680	1.22	3.49	1.82	5.31	2.76	5.41	2.65
10	87300	738	1.31	3.54	1.68	5.22	2.56	5.36	2.80

[a] ϵ is calculated from the absorption spectra of compound **6** at 418 nm, compound **8** at 462 nm, compound **9** at 492 nm and compound **10** at 514 nm. [b] λ_{onset} is the onset of the absorption spectra of compounds. [c] The first reversible half-wave reduction potential (in V vs. Fc/Fc^+) measured in CH_2Cl_2 with a scan rate of 0.1 Vs^{-1} . [d] Estimated from the first reversible half-wave reduction wave using the equation, $E_{\text{A}} = 4.80 + E_{1\text{r}}$. [e] Optical band gap $E_{\text{g}} = 1240/\lambda_{\text{onset}}$. [f] IP energies were estimated from the equation: $\text{IP} = E_{\text{A}} + E_{\text{g}}^{\text{optical}}$, a procedure that neglects the exciton binding energy [g] Calculated at the OT(chloroform)- ω B97XD/6-31G(d,p) level of theory.

Single (two-fold) condensation of BBT bislactams **6** with oxindole **7** decreases the IP value up to ~ 200 meV (400 meV). The electrochemical behavior of **6**, **8**, **9** and **10** were investigated by cyclic voltammetry in dichloromethane solution, with ferrocene / ferrocenium as internal standard and tetrabutylammonium hexafluorophosphate as electrolyte (Figure S12). All the molecules exhibit reversible reduction potential cycles and irreversible oxidation cycles. Two close reversible reduction potentials were exhibited by **6**, with the $E_{\text{pc}}/E_{\text{pa}}$ values for the two peaks $-1.28/-1.22$ and $-1.41/-1.33$ V. Compared with electron rich BBT,²³ the reversible two reduction waves of **6** again demonstrate the distinctly more electron deficient nature of the molecule attributed to the two additional fused lactams. Three reversible reduction potentials of compound **8** could be observed with $E_{\text{pc}}/E_{\text{pa}}$ values of $-1.26/-1.18$, $-1.42/-1.34$, $-1.78/-1.65$ V, respectively. The EAs of these compounds were estimated from the first reversible half-wave reduction potential and the IPs are calculated from the EA and optical band gap, since irreversible oxidation waves of these compounds are observed. The EAs and IPs are 3.55/5.49, 3.58/5.46, 3.49/5.31, 3.54/5.22 eV for **6**, **8**, **9** and **10**, respectively. Note that the EA of BBT (2.5 eV) is much lower than that of **6**,²³ further indicating the large electron withdrawing effect of the additional fused lactams. Extending the conjugation length of the molecule has a more significant effect on the IP whereas the EA remains relatively constant as the molecule size increases, due to its more red shifted nature. The resulting smaller band gaps also explains the red shift absorption spectra of **8**, **9** and **10**. The trends of the band gaps evaluated from the CV are in good agreement with the calculated band gap values obtained from DFT calculations (Table 1). The series of multi lactams oligomers exhibit excellent thermal stability with decomposition temperatures of 360°C for **6**, 340°C for **8**, 345°C for **9**, and 355°C for **10** (Figure S13), respectively.

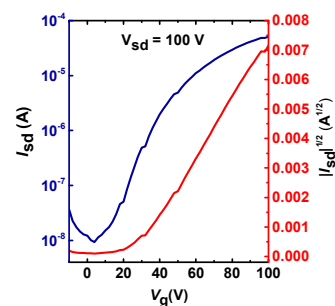


Figure 3: N-type transfer curve of **6**.

BBT bislactam **6** was tested in thin film OFETs with a bottom-contact/bottom-gate (BC/BG) architecture configuration using a Si/SiO₂ substrate containing source and drain electrodes. Thin films were deposited by spin coating and thermally annealed in vacuum at different temperatures to optimize device performance. All the devices were tested in inert atmosphere. The hole and electron

mobilities as a function of the annealing temperatures are summarized in Supporting Information. The devices of **6** exhibit field effect characteristics with an electron-transporting character. The transistors show good drain current saturation and on/off channel current ratios in the range of 10^3 – 10^5 . The maximum electron mobility was calculated directly from the transfer characteristics achieving $0.083 \text{ cm}^2/\text{Vs}$ at an optimized annealing temperature of $250 \text{ }^\circ\text{C}$ (Table S1, Figure 3 and Figure S14), with an average electron mobility of $0.074 \text{ cm}^2/\text{Vs}$. The distinct change from hole transport of BBBT to electron transport behavior of BBBT bisatin, again indicate the strong electron withdrawing ability of the additional fused two lactams. These results also demonstrate that the direct lactam fusion is a useful strategy to design and synthesize novel electron transport materials based other aromatic systems.

In conclusion, a precise series of large and soluble multi-lactam molecules have been prepared and characterized successfully. These oligomers were prepared from a versatile central electron deficient BBBT-bis lactam building block using atom-efficient catalyst-free Knoevenagel condensation and deoxygenated coupling. These larger π -systems of these molecules are locked into a rigid structure by eliminating inter-ring single bonds. These oligomers exhibit broad and high intensity absorption together with long low-wavelength absorption tails. The ability to extend the conjugated system results in red shifted absorption and decreased ionization potentials. The initial thin film transistor results highlight their potential as a new class of materials for organic electronic devices.

Conflicts of interest

“There are no conflicts to declare”.

Acknowledgements

The authors thank the Young National 1000-Talents Program of China, NSF of China (Grant No. 21702240), Marie Curie IEF with FP7 (FP7-PEOPLE-2013-IEF-622187), EC FP7 Project SC2, EC FP7 Project ArtESun, EPSRC Project EP/M005143/1, and ONR Award N-00014-17-1-2208 for financial support.

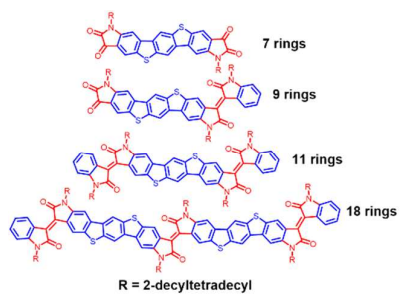
Notes and references

‡ Footnotes relating to the main text should appear here. These might include comments relevant to but not central to the matter under discussion, limited experimental and spectral data.

- [1]. E. Wang, W. Mammo, and M. R. Andersson, *Adv. Mater.*, 2014, **26**, 1801–1826.
- [2]. C. B. Nielsen, M. Turbiez, and I. McCulloch, *Adv. Mater.*, 2013, **25**, 1859–1880.
- [3]. E. Wang, Z. Ma, Z. Zhang, K. Vandewal, P. Henriksson, O. Inganäs, F. Zhang, and M. R. Andersson, *J. Am. Chem. Soc.*, 2011, **133**, 14244–14247.
- [4]. J. Mei, K. R. Graham, R. Stalder, and J. R. Reynolds, *Org. Lett.*, 2010, **12**, 660–663.
- [5]. R. S. Ashraf, A. J. Kronemeijer, D. I. James, H. Sirringhaus, I. McCulloch, *Chem. Commun.*, 2012, **48**, 3939–3941.
- [6]. I. Meager, M. Nikolka, B. C. Schroeder, C. B. Nielsen, M. Planells, H. Bronstein, J. W. Rumer, D. I. James, R. S. Ashraf, A. Sadhanala, P.

Hayoz, J.-C. Flores, H. Sirringhaus, I. McCulloch, *Adv. Funct. Mater.*, 2014, **24**, 7109–7115.

- [7]. W. Yue, M. Nikolka, M. Xiao, A. Sadhanala, C. B. Nielsen, A. J. P. White, H.-Y. Chen, A. Onwubiko, H. Sirringhaus and I. McCulloch, *J. Mater. Chem. C.*, 2016, **4**, 9704–9710.
- [8]. J. Huang, Z. Mao, Z. Chen, D. Gao, C. Wei, W. Zhang, and G. Yu, *Chem. Mater.*, 2016, **28**, 2209–2218.
- [9]. W. Yue, R. S. Ashraf, C. B. Nielsen, E. Collado-Fregoso, M. R. Niazi, S. A. Yousaf, M. Kirkus, H.-Y. Chen, A. Amassian, J. R. Durrant, I. McCulloch, *Adv. Mater.*, 2015, **27**, 4702–4707.
- [10]. N. M. Randell, P. C. Boutin and T. L. Kelly, *J. Mater. Chem. A.*, 2016, **4**, 6940–6945.
- [11]. Y. Jiang, Y. Gao, H. Tian, J. Ding, D. Yan, Y. Geng, and F. Wang, *Macromolecules*, 2016, **49**, 2135–2144.
- [12]. H. Song, Y. Deng, Y. Jiang, H. Tian and Y. Geng, *Chem. Commun.*, 2018, **54**, 782–785.
- [13]. T. Lei, J.-H. Dou, X.-Y. Cao, J.-Y. Wang, and J. Pei, *J. Am. Chem. Soc.*, 2013, **135**, 12168–12171.
- [14]. A. Onwubiko, W. Yue, C. Jellett, M. Xiao, H.-Y. Chen, M. K. Ravva, D. A. Hanifi, A.-C. Knall, B. Purushothaman, M. Nikolka, J.-C. Flores, A. Salleo, J.-L. Bredas, H. Sirringhaus, P. Hayoz, I. McCulloch, *Nat. Commun.*, 2018, **9**, 416.
- [15]. Y. Fukutomi, M. Nakano, J.-Y. Hu, I. Osaka, and K. Takimiya, *J. Am. Chem. Soc.*, 2013, **135**, 11445–11448.
- [16]. Y. Xia, Y. Li, Y. Zhu, J. Li, P. Zhang, J. Tong, C. Yang, H. Li and D. Fan, *J. Mater. Chem. C.*, 2014, **2**, 1601–1604.
- [17]. S. Sun, P. Zhang, J. Li, Y. Li, J. Wang, S. Zhang, Y. Xia, X. Meng, D. Fan and J. Chu, *J. Mater. Chem. A.*, 2014, **2**, 15316–15325.
- [18]. Y. Xia, J. Wang, J. Li, P. Guo, J. Tong, P. Zhang, C. Yang, D. Fan, *Macromol. Chem. Phys.*, 2015, **216**, 733–741.
- [19]. J.-S. Wu, S.-W. Cheng, Y.-J. Cheng, and C.-S. Hsu, *Chem. Soc. Rev.*, 2015, **44**, 1113–1154.
- [20]. T. Zheng, Z. Cai, R. Ho-Wu, S. H. Yau, V. Shaparov, T. Goodson, and L. Yu, *J. Am. Chem. Soc.*, 2016, **138**, 868–875.
- [21]. H. Iino, T. Usui, and J. Hanna, *Nat. Commun.*, 2015, **6**, 6828.
- [22]. H. Ebata, E. Miyazaki, T. Yamamoto, and K. Takimiya, *Org. Lett.*, 2007, **9**, 4499–4502.
- [23]. P. Gao, D. Beckmann, H. N. Tsao, X. Feng, V. Enkelmann, W. Pisulaz, and Klaus Müllen, *Chem. Commun.*, 2008, 1548–1550.
- [24]. V. Coropceanu, J. Cornil, D. A. da Silva Filho, Y. Olivier, R. Stilbey, and J. Brédas, *Chem. Rev.*, 2017, **107**, 926–952.
- [25]. P. Gao, X. Feng, X. Yang, V. Enkelmann, M. Baumgarten, and K. Müllen, *J. Org. Chem.*, 2008, **73**, 9207–9213.
- [26]. Y. Xiong, X. Qiao, H. Wu, Q. Huang, Q. Wu, J. Li, X. Gao, and H. Li, *J. Org. Chem.*, 2014, **79**, 1138–1144;
- [27]. J. Kim, A.-R. Han, J. H. Seo, J. H. Oh, and C. Yang, *Chem. Mater.*, 2012, **24**, 3464–3472.
- [28]. F. Bouchikhi, F. Anizon, and P. Moreau, *Eur. J. Med. Chem.*, 2008, **43**, 755–762.
- [29]. H. Li, F. Sunjoo Kim, G. Ren, E. C. Hollenbeck, S. Subramaniyan, S. and A. Jenekhe; *Angew. Chem. Int. Ed.*, 2013, **52**, 5513–5517.



A series of thienoacene-isoindigo oligomers have been synthesized from novel BBT bislactam. Their opto-electronic and devices characteristics have been investigated.